Available online at www.sciencedirect.com
ScienceDirect
European Journal of Medicinal Chemistry 44 (2009) 165–178
EUROPEAN JOURNAL OF MEDICINAL CHEMISTRY
http://www.elsevier.com/locate/ejmech

Original article

Synthesis and antiproliferative activity of 3-amino-*N*-phenyl-1*H*-indazole-1-carboxamides

Demetrio Raffa [a,*], Benedetta Maggio [a], Stella Cascioferro [a], Maria Valeria Raimondi [a], Domenico Schillaci [a], Giorgio Gallo [a], Giuseppe Daidone [a], Salvatore Plescia [a], Fiorella Meneghetti [b], Gabriella Bombieri [b], Antonietta Di Cristina [c], Rosaria M. Pipitone [c], Stefania Grimaudo [c], Manlio Tolomeo [c]

[a] *Dipartimento di Chimica e Tecnologie Farmaceutiche, Università degli Studi di Palermo, Via Archirafi, 32, 90123 Palermo, Italy*
[b] *Istituto di Chimica Farmaceutica e Tossicologica ''P. Pratesi'', Università degli Studi di Milano, Viale Abruzzi, 42, 20131 Milano, Italy*
[c] *Divisione di Ematologia e Servizio AIDS, Policlinico Universitario ''Paolo Giaccone'', Università degli Studi di Palermo, Via del Vespro, 129, 90127 Palermo, Italy*

Received 7 August 2007; received in revised form 20 February 2008; accepted 20 March 2008
Available online 8 April 2008

Abstract

A series of new 3-amino-*N*-phenyl-1*H*-indazole-1-carboxamides **10** have been prepared from commercially available phenyl isocyanate precursors **8** and 3-aminoindazole **9**. Some of the synthesized compounds were evaluated for their in vitro antineoplastic activity against 60 human cell lines derived from seven clinically isolated cancer types (lung, colon, melanoma, renal, ovarian, brain, and leukemia) according to the NCI standard protocol. The test results indicated that 3-amino-1*H*-indazole-1-carboxamides **10** were endowed with an interesting antiproliferative activity. The most active compounds of this series, **10d**,**e**, were able to inhibit cell growth of many neoplastic cell lines at concentrations lower than 1 μM (0.0153 μM in SR leukemia) causing a block in G0–G1 phase of cell cycle. Analysis of pRb expression showed that these two compounds increased the ratio between underphosphorylated pRb and total pRb. The X-ray structure of **10w**, confirmed the 3-amino-*N*-phenyl-1*H*-indazole-1-carboxamide structure of compounds **10**.

Keywords: 1*H*-Indazole-1-carboxamides; Crystallographic study; G0–G1 arrest; pRb

1. Introduction

Indazole nucleus represents a very attractive scaffold to obtain new molecules endowed with antineoplastic activity. As examples (Fig. 1), *N*2-(substituted benzyl)-3-(4-methylphenyl)-2*H*-indazoles **1** exhibit antiangiogenic activity [1] and 4-methoxy-*N*-(3-chloro-indazol-7-yl)benzenesulfonammide **2** possesses antiproliferative activity against L1210 murine leukemia cells [2]. Moreover, *N*-[4-(3-amino-1*H*-indazol-4-yl)-phenyl]-*N*′-(3-methylphenyl)-urea (ABT-869) **3** has shown significant tumor growth inhibition in multiple preclinical animal models [3], and pyrimido[1,2-*b*]indazoles **4** are potential anticancer agents against A-549 cell line [4]. Finally, lonidamine **5**, 1-(2,4-dichlorobenzyl)-1*H*-indazole-3-carboxylic acid, is a relatively new non-conventional anticancer drug that selectively inhibits the energy metabolism of neoplastic cells and increases the cell membranes permeability [5].

Recently our research group has reported the synthesis of new indazole derivatives owing to their interesting antiproliferative activity. In particular, we have linked the indazole moiety to the quinazolin-4(3*H*)-one and benzotriazin-4(3*H*)-one nuclei with the aim to evaluate the pharmacological profile of the indazol-3-yl and indazol-5-yl derivatives [6,7]. The pharmacological screening showed that 3-(indazol-3-yl)-7-chloro-2-ethyl-quinazolin-4(3*H*)-one **6** was the most active

* Corresponding author. Tel.: +39 091 6236117.
E-mail address: demraffa@unipa.it (D. Raffa).

0223-5234/$ - see front matter © 2008 Elsevier Masson SAS. All rights reserved.
doi:10.1016/j.ejmech.2008.03.023

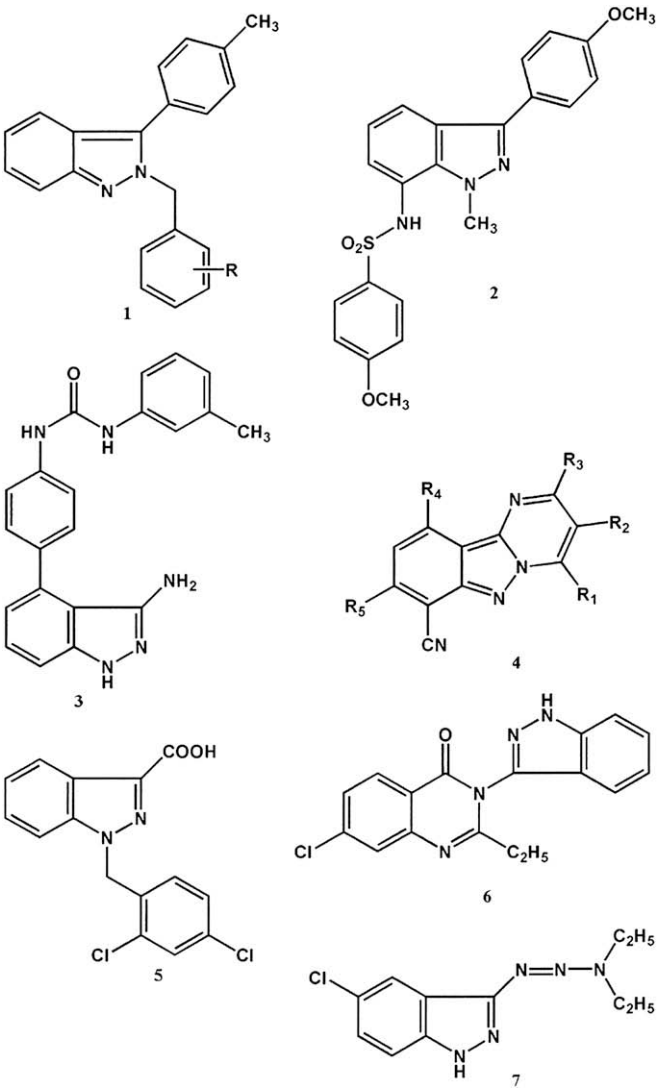

Fig. 1. Chemical structure of some examples of antineoplastic agents which posses the indazole nucleus.

derivative with a GI_{50} recorded on K562 and K562-R cell lines of 10.7 and 11.7 μM, respectively. Moreover, we synthesized some new triazenoindazoles which showed in vitro cytotoxic activity against K562, HL-60, L1210 and MCF7 cell lines. Among the tested compounds, 3-(3′,3′-diethyltriazeno)-5-chloroindazole **7** was the most active one against all the cell lines [8]. These data clearly indicated that triazenoindazoles act in vitro with a different mechanism with respect to that of dacarbazine which is generally based on metabolic activation in vivo [9].

Finally, owing to our interest to the chemistry and pharmacology of indazole derivatives, and considering that the chemical class of 3-amino-*N*-phenyl-1*H*-indazole-1-carboxamides **10** possesses some novel structural elements, we decided to investigate whether these compounds can give rise to biological activity. Later these were, therefore, synthesized and evaluated for their antineoplastic activity. The most active compounds were evaluated for their effects on cell cycle distribution in K562 cells as well as on the underphosphorylated and total retinoblastoma protein (pRb) ratio.

Due to the presence of the indazole nucleus, the *N*-phenyl-3-(phenylureido)-1*H*-indazole-1-carboxamides by-products **11** and the 1-(1*H*-indazol-3-yl)-3-phenylureido derivatives **12** (see Scheme 1) were also considered as potential antiproliferative agents.

2. Chemistry

The synthesis [10] of the 3-amino-*N*-phenyl-1*H*-indazole-1-carboxamide derivatives **10** started from the commercially available phenyl isocyanate precursors **8** and 3-aminoindazole **9** [11]. As reported in Fig. 2, this reaction should give all the possible substitution products, that is the monosubstituted derivatives **10**, **12** and **13** as well as the disubstituted ones **11** and **14**. However, as outlined in Scheme 1, only the products **10**–**12** were obtained owing to the experimental conditions: (A) refluxing of a suitable substituted phenyl isocyanate **8** with 3-aminoindazole **9** (isocyanate:indazole 1:1) in tetrahydrofuran (1–6 h); (B) refluxing of a suitable substituted phenyl isocyanate **8** with 3-aminoindazole **9** (isocyanate:indazole 2:1) in tetrahydrofuran (1–6 h); and (C) stirring at 25 °C of a suitable substituted phenyl isocyanate **8** and the 3-aminoindazole **9** (isocyanate:indazole 1:1) in tetrahydofuran for 24 h.

The attempt to obtain derivatives **10** from **8a**,**d** and **9** according to the procedure A failed, affording a complex multicomponent mixture. Later on, the mixture was monitored for the presence of compounds **10a**,**d** by TLC using the authentic specimens of **10a**,**d**, **11a**,**d** and **12a**,**d** obtained from the procedures B and C; TLC revealed the presence of small amounts of **10a**,**d** and **11a**,**d** in the reaction mixture.

By varying the ratio of reactants as outlined in procedure B, the workup and purification of the reaction mixture afforded one of the compounds **11** or **12** as the major product. In particular, isocyanates **8a**,**d**–**i**,**l**,**n**,**q**–**s** gave the compounds **11a**,**d**–**i**,**l**,**n**,**q**–**s** whereas **8b**,**c**,**o**,**p** the 1-(1*H*-indazol-3-yl)-3-phenylureido derivatives **12b**,**c**,**o**,**p**. Moreover, attempts to obtain derivatives **10** by hydrolysis of derivatives **11a**,**d**–**i**,**l**,**n**,**q**,**r** gave the 1-(1*H*-indazol-3-yl)-3-phenylureido derivatives **12a**,**d**–**i**,**l**,**n**,**q**,**r**.

Finally, according to the procedure C, stirring at room temperature for 24 h a mixture of substituted phenyl isocyanate **8** and 3-aminoindazole **9** in tetrahydofuran allowed us to obtain the expected derivatives **10**.

In principle this reaction should give both the 3-amino-*N*-phenyl-1*H*-indazole-1-carboxamide derivative **10** and the 3-amino-*N*-phenyl-2*H*-indazole-2-carboxamide isomer **13** (Fig. 2). The analytical as well as spectroscopical data of the reaction products well correlated with both the structures **10** and **13**, therefore, for a conclusive attribution of the 3-amino-*N*-phenyl-1*H*-indazole-1-carboxamide structure **10**, compound **10w** was analyzed by X-ray diffraction techniques (Fig. 3).

On the basis of the crystallographic results of **10w** and considering the sterical hindrance of the phenylureido moiety in the position 3, we have attributed to the product of diacylation the 1*H*-indazole-1-carboxamide structure **11** instead of 2*H*-indazol-2-carboxamide one **14**.

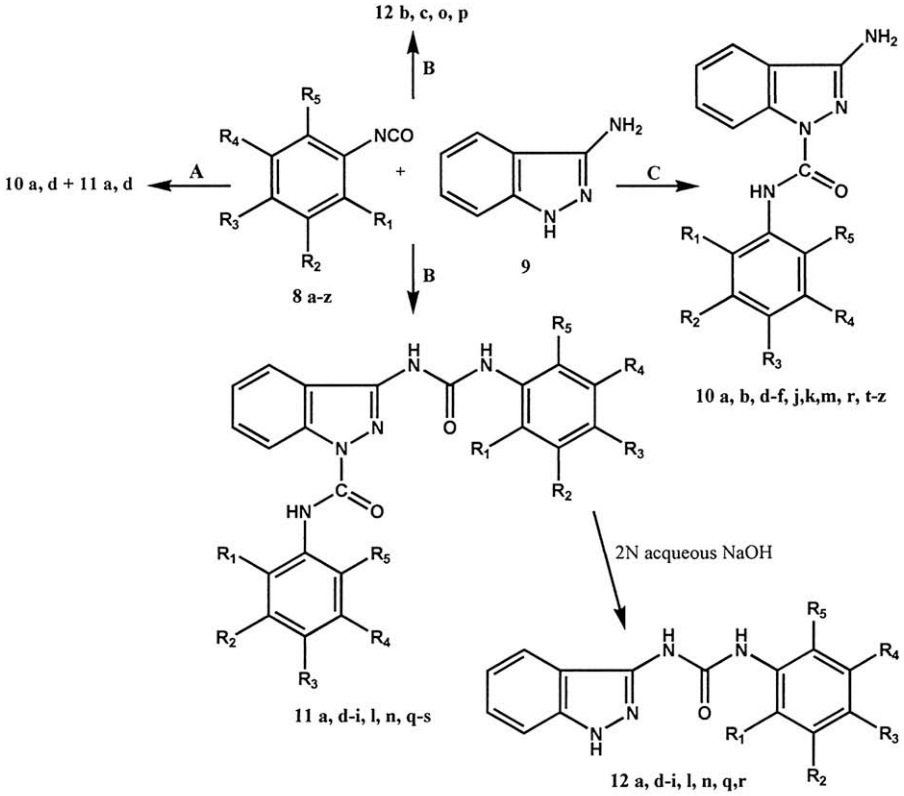

	R_1	R_2	R_3	R_4	R_5
a	F	H	H	H	F
b	Cl	H	H	Cl	H
c	H	H	C_6H_5O	H	H
d	H	H	$C_6H_5CH_2$	H	H
e	H	H	C_4H_9O	H	H
f	H	H	CH_3CO	H	H
g	H	H	OCH_3	H	H
h	H	H	OCF_3	H	H
i	F	H	H	CF_3	H
j	Cl	H	NO_2	H	H
k	C_4H_4		H	H	H
l	OCF_3	H	H	H	H
m	CH_3	H	H	NO_2	H

	R_1	R_2	R_3	R_4	R_5
n	H	Cl	Cl	H	H
o	H	H	NO_2	H	H
p	CH_3	H	NO_2	H	H
q	H	H	Br	H	H
r	C_2H_5O	H	H	H	H
s	H	H	C_4H_9	H	H
t	$C_6H_5CH_2$	H	H	H	H
u	OCH_3	H	H	NO_2	H
v	H	OCH_3	OCH_3	H	H
w	H	H	$C_6H_5CH_2O$	H	H
x	OCH_3	H	OCH_3	H	H
y	OCH_3	H	H	H	H
z	OCH_3	H	H	OCH_3	H

A isocyanate/indazole 1:1, reflux, 1-6 h
B isocyanate/indazole 2:1, reflux, 1-6 h
C isocyanate/indazole 1:1, T=25°, 24h

Scheme 1. Synthetic pathway for the formation of the compounds **10**, **11** and **12**.

The structures of the new compounds were characterized by analytical and spectroscopic measurements. The ^{1}H NMR spectra of **10** showed both the NH and NH_2 signals of the 3-amino-*N*-phenyl-1*H*-indazole-1-carboxamide structure. In fact, the 1-carboxamide NH proton appeared as singlet at 8.99–9.89 δ, while the amino protons were found as a broad singlet at 6.31–6.70 δ. ^{1}H NMR spectra of **11** are consistent with an *N*-phenyl-3-(phenylureido)-1*H*-indazole-1-carboxamide structure. The 1-carboxamide NH protons appeared as singlets at 9.42–10.11 δ, while the phenylureido NH protons were found at 9.67–10.26 δ and 10.10–10.70 δ, respectively. Finally, the ^{1}H NMR spectra of **12** demonstrated the 1-(1*H*-indazol-3-yl)-3-phenylureido structure. The 1*H*-indazole NH proton appeared as a singlet at 12.47–12.69 δ, while the phenylureido NH protons were found at 9.30–10.30 δ and 9.79–10.72 δ, respectively.

3. Crystallography

The crystal structure of **10w** is shown in Fig. 3 as ORTEP [12] view. The overall conformation of the molecule is defined by the torsion angles τ_1 C(12)–O(2)–C(15)–C(16) of 76(1)°, τ_2 C(14)–C(9)–N(4)–C(8) of 29(1)° and τ_3 C(21)–C(16)–C(15)–O(2) of 50(1)°, showing a significant tilting of the distal phenyl moiety with respect to the rest of the molecule. The indazole ring has an inclination of 35(1)° compared to the proximal phenyl group (centroids distance 6.9(1) Å) and of 80(1)° with the distal phenyl group (centroids distance 10.9(1) Å). The two phenyl groups are almost perpendicular with a dihedral angle of 81(1)°(centroids distance 5.1(1) Å). The main packing determinants are hydrogen bonds N(3)–H···O(2)′, with distance of 2.18(1) Å and angle 163(1)° (at 3/2−*x*, 1/2−*y*, 1/3−*z*) with consequent formation of dimers involving centrosymmetrically related molecules. Further

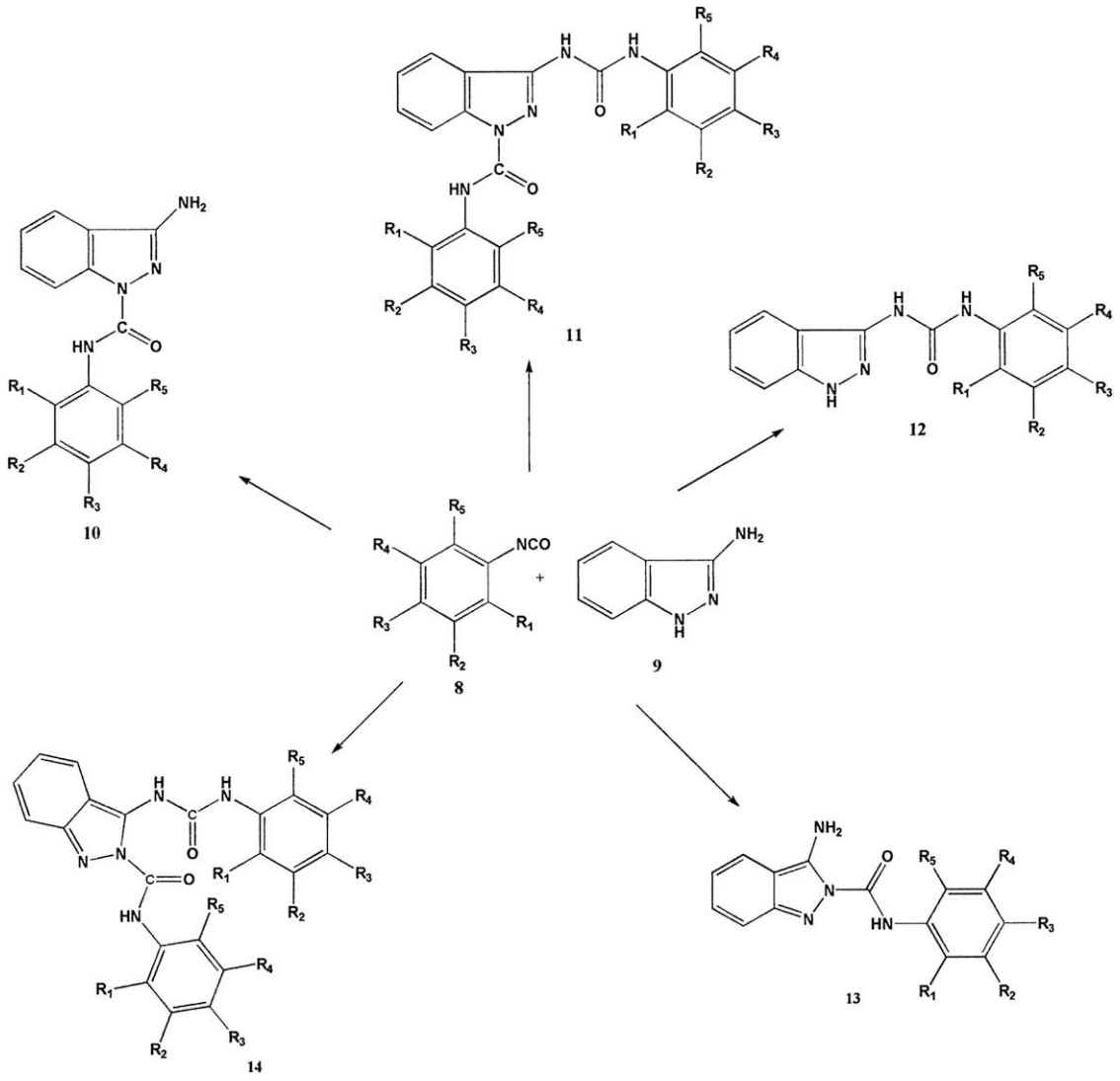

Fig. 2. Possible substitution products that can be derived from compounds **8** and **9**.

interactions between C(11)–H···N(1)′ at 2.73(1) Å with angle 133(1)° contribute to the dimer's stability (Fig. 3).

4. Pharmacological results

4.1. Tumor cell line screen

3-Amino-*N*-phenyl-1*H*-indazole-1-carboxamides **10a**,**d**,**e**, **v**,**y**, *N*-phenyl-3-(phenylureido)-1*H*-indazole-1-carboxamide **11d**, and the 1-(1*H*-indazol-3-yl)-3-phenylureido derivatives **12g**,**i**,**l** were selected by the National Cancer Institute (NCI) to evaluate their in vitro antiproliferative activity against 60 human cell lines derived from seven clinically isolated cancer types (lung, colon, melanoma, renal, ovarian, brain, and leukemia) according to the NCI standard protocol [13].

The antitumor activity is given by three parameters for each cell line; GI_{50} (compound's molar concentration inhibiting 50% net cell growth), TGI (compound's molar concentration for total inhibition of net cell growth), and LC_{50} (compound's molar concentration inducing 50% net cell death). The GI_{50} values for the test compounds were reported in the Table 1.

4.2. Cell cycle analysis

The effects of the most active compounds (**10d**,**e**,**y**, **12i**,**l**) on cell cycle distribution were analysed in K562 cells. Cells were cultured for 24 h in the presence of each compound at the GI_{50} concentration evaluated after 24 h of treatment (**10d** 1.20 μM, **10e** 15.9 μM, **10y** 180 μM, **12i** 140 μM and **12l** 42.7 μM). Flow cytometric analyses of cell cycle, carried out as described in Section 7, are reported in Fig. 4. Compounds **10y**, **12i**,**l** induced a recruitment of cells in S and G2M phase while compounds **10d**,**e** caused a marked increase of cells in G0–G1 phase and a decrease of cells either in S or G2–M phase. Since most of chemotherapeutic drugs act on S or G2M phase and are ineffective in G0–G1 phase, we considered compounds **10d**,**e** of interest for deep investigations.

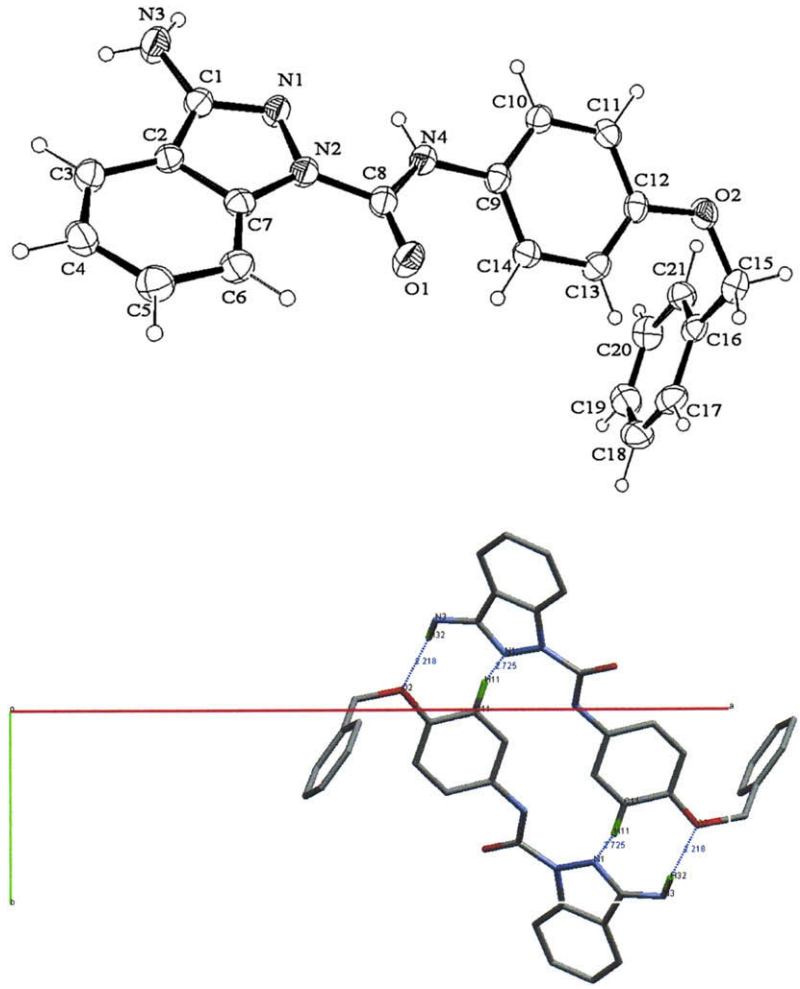

Fig. 3. Left: ORTEP [12] view of the compound **10w**, showing the atom-numbering scheme (ellipsoids are at 40% probability and H-atoms are shown as spheres of arbitrary radius). Right: intermolecular interactions along the crystallographic *c* axis. Selected bond lengths [Å] and angles [°]: O(1)–C(8), 1.212(4); O(2)–C(12), 1.384(4); O(2)–C(15), 1.439(5); N(1)–C(1), 1.313(5); N(1)–N(2), 1.403(4); N(2)–C(7), 1.388(5); N(2)–C(8), 1.399(5); N(3)–C(1), 1.372(5); N(4)–C(8), 1.357(5); N(4)–C(9), 1.414(5); O(1)–C(8)–N(4), 126.9(4); O(1)–C(8)–N(2), 121.2(4); N(1)–N(2)–C(7), 110.8(3); N(1)–N(2)–C(8), 120.3(3); N(1)–C(1)–N(3), 121.0(4); N(2)–C(8)–N(4), 111.9(3); N(3)–C(1)–C(2), 126.8(4); N(2)–N(1)–C(1), 105.6(3).

4.3. Effects on retinoblastoma protein (pRb)

The retinoblastoma gene encodes a nuclear phosphoprotein (pRb) expressed in the majority of vertebrates' normal cells and acts as a tumor suppressor factor which plays a key role in the control of cell division [14]. The pRb underphosphorylated form is mainly found in resting cells, whereas the highly phosphorylated forms are present in proliferating cells. Growth factors act to promote cells through the G1 and S phase of cell cycle and, during this time, pRb undergoes sequential phosphorylation. The pRb underphosphorylated form binds to critical regulatory proteins (including E2F) and represses the transcription of genes involved in cell cycle progression from the G1 to the S phase [15]. Fig. 5 shows the effects of **10d**,**e** on total Rb and underphosphorylated pRb levels in K562 cells.

Flow cytometric analyses of pRb and underphosphorylated pRb were carried out as described in Section 7. Compounds **10d**,**e** caused a decrease of total pRb but the level of underphosphorylated pRb was similar to that of the control. Therefore, in both cases the ratio between underphosphorylated pRb and total pRb was increased.

5. Discussion

All the compounds **10a**,**d**,**e**,**v**,**y**, **11d**, **12g**,**i**,**l** tested by NCI were found to possess low cytotoxicity. On the other hand, they turn out to be inhibitor of cell growth with GI_{50} values ranging from 0.0153 to 98.8 μM with the exception of **12g** which was totally inactive (Table 1). Among these, the best antiproliferative agent resulted compound **10d** which showed antiproliferative activity against every type of tumor cell lines investigates. As it can be seen in Table 2 it was particularly active against all kinds of leukemia and mostly active against some other cell lines such as non-small cell lung (NCI-H460, NCI-H522), colon cancer (HTC-15, HT29, KM12), CNS cancer (SF-295, SF-539), melanoma (LOXIMVI, M14, SK-MEL-5, UACC-62), renal cancer (ACHN, UO-31), prostate cancer (DU-145) and breast cancer (MCF7, MDA-MB-231/ATCC, MDA-MB-435, T-47D). Good activity has also been shown

Table 1
Compound's molar concentration inhibiting 50% net cell growth (GI_{50}, μM) of **10a**,**d**,**e**,**v**,**y**, **11d**, **12g**,**i**,**l** against 60 human cell lines derived from seven clinically isolated cancer types

Cancer types	Panel/cell line	**10a**	**10d**	**10e**	**10y**	**10v**	**11d**	**12g**	**12i**	**12l**
Leukemia	CCRF-CEM	nt	nt	0.213	>100	36.7	nt	59.6	nt	nt
	HL-60 (TB)	33.2	0.466	2.23	47.2	27.9	>100	>100	>100	17.9
	K-562	<100	1.20	15.9	>100	41.2	40.5	>100	>100	42.7
	MOLT-4	32.7	0.636	4.48	54.0	39.4	63.2	>100	>100	59.1
	RPMI-8226	16.1	1.86	2.72	86.0	21.1	>100	>100	>100	52.0
	SR	12.9	0.0153	16.0	92.5	29.3	16.3	>100	55.4	0.0489
Non-small cell lung cancer	A549/ATCC	48.5	12.9	23.5	>100	45.8	>100	>100	>100	15.7
	EKVX	84.0	11.2	13.3	44.8	54.1	>100	>100	>100	48.2
	HOP-62	51.0	13.7	20.8	>100	75.2	59.7	>100	>100	19.6
	HOP-92	17.3	14.2	18.6	30.2	24.6	18.0	>100	>100	12.9
	NCI-H226	98.5	13.5	21.2	>100	83.1	>100	>100	>100	26.1
	NCI-H23	95.6	16.8	19.4	>100	83.5	>100	>100	>100	50.0
	NCI-H322M	<100	27.8	20.6	>100	>100	>100	>100	>100	81.6
	NCI-H460	33.4	0.408	15.7	78.9	34.5	>100	>100	>100	15.0
	NCI-H522	55.1	2.90	27.4	49.5	34.9	>100	>100	>100	33.9
Colon cancer	COLO 205	<100	13.4	13.9	>100	85.9	>100	>100	>100	71.8
	HCC-2998	95.8	4.27	19.0	66.2	61.1	>100	>100	>100	55.9
	HCT-116	34.8	7.03	19.9	>100	43.5	>100	>100	>100	16.2
	HCT-15	40.9	1.08	15.5	73.6	44.1	>100	>100	>100	36.2
	HT29	74.6	2.39	13.5	>100	48.2	>100	>100	>100	26.1
	KM12	86.2	2.94	11.3	39.1	67.9	>100	>100	>100	23.4
	SW-620	38.3	3.62	18.3	>100	>100	>100	>100	>100	36.7
CNS cancer	SF-268	36.2	4.66	25.8	>100	49.6	75.6	>100	>100	16.2
	SF-295	54.8	0.530	21.7	56.6	37.6	>100	>100	>100	39.0
	SF-539	31.4	0.495	17.8	60.9	95.9	>100	>100	>100	30.5
	SNB-19	<100nt	22.8	42.7	>100	>100	>100	>100	>100	78.3
	SNB75		17.0	28.6	37.0	30.6	33.8	>100	40.1	17.5
	U251	96.1	13.9	30.5	98.7	61.7	70.2	>100	>100	31.1
Melanoma	LOX IMVI	49.3	0.477	12.2	92.1	49.3	71.0	>100	>100	22.5
	MALME-3M	<100	19.2	14.7	>100	>100	>100	>100	>100	76.9
	M14	74.7	0.772	18.6	>100	64.9	>100	>100	>100	22.5
	SK-MEL-2	<100	36.4	nt	nt	37.2	>100	>100	>100	81.4
	SK-MEL-28	56.3	11.5	32.6	>100	>100	>100	>100	>100	42.2
	SK-MEL-5	39.7	2.22	15.2	>100	27.9	>100	>100	>100	28.7
	UACC-257	71.7	10.0	29.2	>100	73.6	>100	>100	>100	47.2
	UACC-62	43.9	0.353	14.7	>100	52.3	41.6	>100	>100	31.7
Ovarian cancer	IGROV1	7.70	6.98	35.5	27.3	18.1	>100	>100	0.758	4.59
	OVCAR-3	65.7	6.23	18.8	>100	92.0	>100	>100	>100	90.8
	OVCAR-4	57.8	10.7	30.7	>100	63.2	>100	>100	>100	37.7
	OVCAR-5	<100	31.3	20.0	>100	45.5	>100	>100	>100	34.3
	OVCAR-8	44.2	21.9	35.9	>100	39.7	>100	>100	>100	29.6
	SK-OV-3	<100	36.9	44.0	>100	>100	>100	>100	>100	>100
Renal cancer	786-0	<100	3.76	21.0	>100	>100	>100	>100	>100	38.7
	A498	31.4	16.7	19.0	>100	30.3	82.4	>100	>100	>100
	ACHN	50.1	1.69	22.8	>100	58.3	>100	>100	>100	31.1
	CAKI-1	45.3	21.1	28.3	>100	>100	>100	>100	>100	31.0
	RXF 393	20.2	22.2	29.6	45.7	95.2	30.4	>100	>100	24.3
	SN12C	<100	12.9	23.1	>100	>100	>100	>100	>100	72.5
	TK-10	<100	27.2	24.2	74.3	92.4	>100	>100	>100	37.9
	UO-31	18.6	0.347	17.5	>100	28.5	>100	>100	>100	17.4
Prostate cancer	PC-3	<100	13.5	14.9	83.1	35.5	>100	>100	>100	31.4
	DU-145	62.3	1.02	25.0	>100	73.1	80.0	>100	>100	51.7
Breast cancer	MCF7	60.0	0.555	14.5	0.269	29.5	>100	>100	18.2	1.75
	NCI/ADR-RES	56.5	7.87	23.7	90.7	37.6	>100	>100	>100	44.2
	MDA-MB-231/ATCC	98.8	0.847	13.8	46.1	53.6	47.1	>100	>100	17.9
	HS 578T	73.0	17.2	20.2	33.8	43.3	74.2	>100	>100	19.4
	MDA-MB-435	54.9	2.82	19.1	>100	>100	>100	>100	>100	51.5
	BT-549	28.8	13.5	14.0	28.0	25.9	>100	>100	>100	76.4
	T-47D	68.7	1.55	14.8	>100	33.0	>100	>100	0.215	37.5

nt: Not tested.

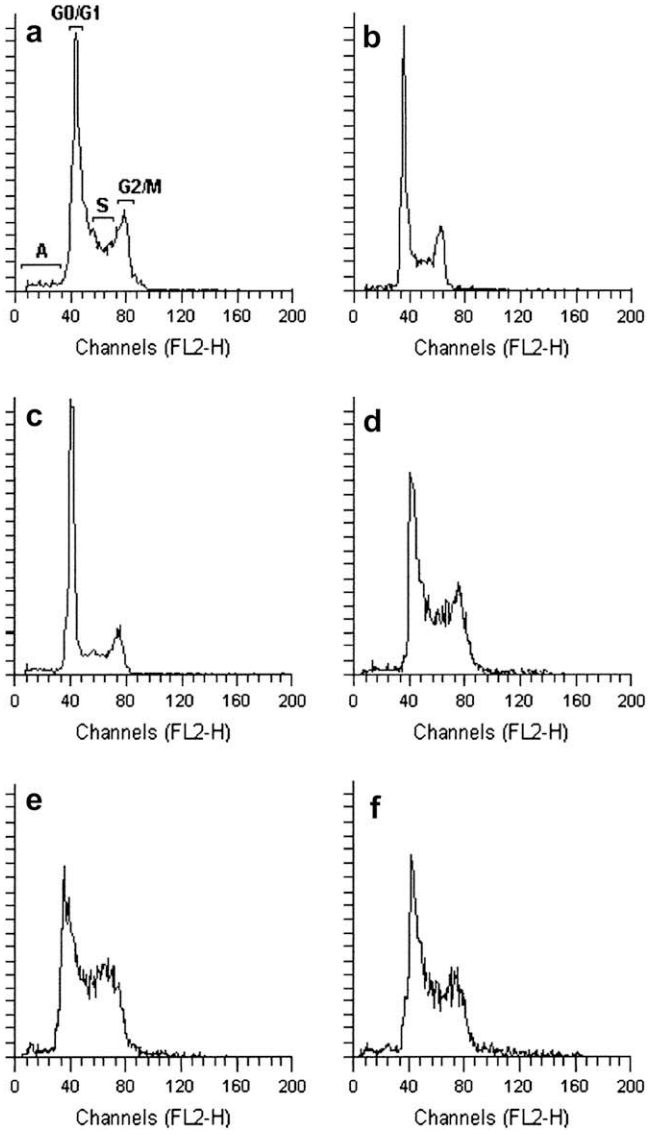

Fig. 4. Effects of compounds **10d** (b), **10e** (c), **10y** (d), **12i** (e), **12l** (f) on DNA content/cell following the treatment of K562 cells for 24 h. The cells were cultured without any compound (a) or with each compound used at the concentration corresponding to the GI_{50}. Cell cycle distribution was analyzed by the standard propidium iodide procedure as described in Section 7. Sub-G0–G1 (A), G0–G1, S, and G2–M cells are indicated in panel a.

from compound **10e** even if it resulted less active with respect to **10d**. In fact, it was efficacious against the leukemic cell lines with particular respect to CCRF-CEM, HL-60, MOLT-4 and RPMI-8226 (Table 3) being a micromolar inhibitor in all the other ones (Table 1).

Moreover, **10d,e** were the only compounds endowed of significant TGI values ranging from 1.25 to 97.9 μM against almost all cell lines of the NCI panel and, in some cases, of LC_{50} value ranging from 34.3 to 96.4 μM (Tables 2 and 3).

Significant results were also showed from the compounds **10y**, **12i,l** although only in a very limited numbers of cell lines; with respect to leukemic cell line SR compounds **12l** showed a remarkable activity, the compound **10y** was very active against MCF7 while the IGROV1 and T-47D were inhibited by **12i** (Table 4).

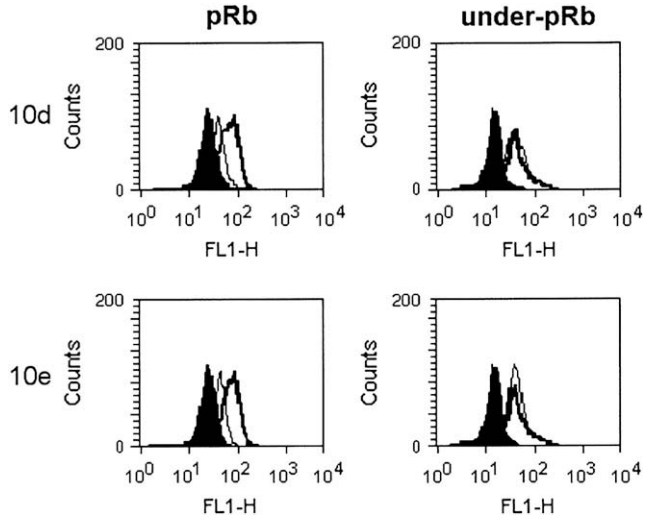

Fig. 5. Effects of compounds **10d,e** on total pRb or underphosphorylated pRb (under-P-pRb) expressions. The cells were cultured without any compounds or with each compound (10d = 14 μM, 10e = 34 μM). Black filled line: cells stained with an isotype monoclonal antibody (control); thick line: cells stained with an anti-pRb or an anti-underphosphorylated-pRb monoclonal antibody; thin line: cells stained with an anti-pRb or an anti-underphosphorylated-pRb monoclonal antibody after 24 h treatment with each compound.

The effects of **10d,e** on cell cycle distribution showed how these compounds induced a marked recruitment of cells in G0–G1. Concerning the effects on retinoblastoma protein (pRb), compounds **10d,e** caused a decrease in total pRb without any modification of the underphosphorylated pRb level.

Table 2
In vitro antiproliferative activity (μM) against the cell lines in which the compound **10d** resulted mostly active

Cancer types	Panel/cell line	**10d**		
		GI_{50}	TGI	LC_{50}
Leukemia	HL-60 (TB)	0.466	15.2	54.9
	K-562	1.20	33.8	>100
	MOLT-4	0.636	20.4	>100
	RPMI-8226	1.86	25.8	84.0
	SR	0.0153	82.2	34.8
Non-small cell lung cancer	NCI-H460	0.408	13.0	84.6
	NCI-H522	2.90	>100	>100
Colon cancer	HCT-15	1.08	>100	>100
	HT29	2.39	17.6	56.3
	KM12	2.94	>100	>100
CNS cancer	SF-295	0.530	>100	>100
	SF-539	0.495	5.36	>100
Melanoma	LOX IMVI	0.477	16.1	61.5
	M14	0.772	>100	>100
	SK-MEL-5	2.22	8.64	34.3
	UACC-62	0.353	>100	>100
Renal cancer	ACHN	1.69	33.4	>100
	UO-31	0.347	>100	>100
Prostate cancer	DU-145	1.02	28.3	>100
Breast cancer	MCF7	0.555	8.82	89.1
	MDA-MB-231/ATCC	0.847	43.9	>100
	MDA-MB-435	2.82	>100	>100
	T-47D	1.55	>100	>100

Table 3
In vitro antiproliferative activity (μM) of **10e**

Cancer type	Panel/cell line	**10e**		
		GI_{50}	TGI	LC_{50}
Leukemia	CCRF-CEM	0.213	17.5	>100
	HL-60 (TB)	2.23	30.4	>100
	MOLT-4	4.48	46.2	>100
	RPMI-8226	2.72	30.8	>100

Table 4
In vitro antiproliferative activity (μM) of **10y**, **12i** and **12l**

Compound	Cancer types	Panel/cell line	GI_{50}	TGI	LC_{50}
10y	Breast	MCF7	0.269	64.6	>100
12i	Ovarian	IGROV1	0.758	>100	>100
	Breast	T-47D	0.215	>100	>100
12l	Leukemia	SR	0.0489	24	>100

This suggests that they could act by inducing a decrease in the phosphorylated form of pRb. A similar activity has recently been described for compound tyrphostin AG1024 in melanoma cells [16]. Tyrphostin AG1024 caused the loss of phosphorylated forms of pRb that was not associated with suppression of cyclin-dependent kinases 2 and 4 activity but rather with proteasomal and nonproteasomal degradation of phosphorylated pRb. Because mutations in the retinoblastoma gene (RB-1) have been described in a wide variety of neoplasm, and constitutive phosphorylation/inactivation of pRb has been implicated in conferring uncontrolled growth to many neoplastic cells [17], compounds able to decrease the level of phosphorylated pRb could be of interest in the treatment of different malignancies.

6. Conclusion

3-Amino-*N*-phenyl-1*H*-indazole-1-carboxamides **10** here described were primarily designed considering the well-known biological activity of the indazole nucleus and their structural novelty. The effects on cell cycle distribution showed how these compounds induced a marked recruitment of cells in G0–G1 but not in G2–M. This is a very encouraging result considering that currently, drugs capable of blocking and/or killing cancer cells in the G0–G1 phase are considered of primary importance because most chemotherapeutic drugs used in the treatment of malignancies act in the S or G2–M phase of the cell cycle but not in G0–G1. Thus, a variable percentage of cells in G0–G1 could escape from the cytotoxic effects of the therapy (minimal residual disease) causing a relapse of the disease months or years later [18–24].

7. Experimental protocols

7.1. Chemistry

7.1.1. General

Reaction progress was monitored by TLC on silica gel plates (Merck 60, F_{254}, 0.2 mm). Organic solutions were dried over Na_2SO_4. All melting points were determined on a Büchi 530 capillary apparatus and are uncorrected. IR spectra were recorded with a Perkin Elmer Spectrum RXI FT-IR System spectrophotometer in KBr disc. ^{1}H NMR spectra were obtained with a Bruker AC-E 250-MHz spectrometer (tetramethylsilane as an internal standard): chemical shifts are expressed in δ values (ppm). Merck silica gel (Kiesegel 60/230–400 mesh) was used for flash chromatography columns. Microanalyses (C, H, N) performed at REDOX snc Monza (MI) Italy are within ±0.4% of the theoretical values. Yields refer to purified products and are not optimized.

7.1.2. Starting material

All phenyl isocyanates **8a–z** were purchased from Aldrich Chemical Company and were used as received.

7.1.3. Synthesis of 3-amino-N-phenyl-1H-indazole-1-carboxamides *10*

7.1.3.1. General method. A mixture of 14 mmol of substituted phenyl isocyanate **8** and 14 mmol of 3-aminoindazole **9** in 10 ml of THF was stirred at room temperature for 24 h. At the completion of the reaction the solvent was removed under reduced pressure, the solid residue was washed with ethanol and then crystallized from a suitable solvent.

*7.1.3.1.1. 3-Amino-N-(2,6-difluorophenyl)-1H-indazole-1-carboxamide **10a**.* 2,6-Difluorophenyl isocyanate **8a** was allowed to react with 3-aminoindazole **9** as described in Section 7.1.3.1 to give **10a**. Purified by flash chromatography on silica gel [25] with chloroform as eluant, and crystallized from dioxane, 65% yield; mp 165–168 °C; I.R. (KBr, cm^{-1}) 3486, 3359 (NH, NH_2), 1688 (CO); ^{1}H NMR (DMSO) δ 6.40 (s, 2H, NH_2, exchangeable); 7.19–8.15 (a set of signals, 7H, aromatic protons); 9.30 (s, 1H, NH, exchangeable). Anal. ($C_{14}H_{10}F_2N_4O$) C, H, N.

*7.1.3.1.2. 3-Amino-N-(2,5-dichlorophenyl)-1H-indazole-1-carboxamide **10b**.* 2,5-Dichlorophenyl isocyanate **8b** was allowed to react with 3-aminoindazole **9** as described in Section 7.1.3.1 to give **10b**. Purified by preparative TLC (silica gel plate, layer thickness 2 mm, chloroform as eluant), and crystallized from ethanol, 45% yield; mp 185–188 °C; I.R. (KBr, cm^{-1}) 3439, 3341 (NH, NH_2), 1697 (CO); ^{1}H NMR (DMSO) δ 6.67 (s, 2H, NH_2, exchangeable); 7.21–8.40 (a set of signals, 7H, aromatic protons). 9.47 (s, 1H, NH, exchangeable). Anal. ($C_{14}H_{10}Cl_2N_4O$) C, H, N.

*7.1.3.1.3. 3-Amino-N-(4-benzylphenyl)-1H-indazole-1-carboxamide **10d**.* 4-Benzylphenyl isocyanate **8d** was allowed to react with 3-aminoindazole **9** as described in Section 7.1.3.1 to give **10d**. The solid collected was crystallized from dioxane, 26% yield; mp 158–160 °C; I.R. (KBr, cm^{-1}) 3456, 3344 (NH, NH_2), 1699 (CO); ^{1}H NMR (DMSO) δ 3.91 (s, 2H, CH_2); 6.35 (s, 2H, NH_2, exchangeable); 7.18–8.19 (a set of signals, 13H, aromatic protons). 9.44 (s, 1H, NH, exchangeable). Anal. ($C_{21}H_{18}N_4O$) C, H, N.

*7.1.3.1.4. 3-Amino-N-(4-butoxyphenyl)-1H-indazole-1-carboxamide **10e**.* 4-Butoxyphenyl isocyanate **8e** was allowed to react with 3-aminoindazole **9** as described in Section

7.1.3.1 to give **10e**. The solid collected was crystallized from ethanol, 98% yield; mp 138–141 °C; I.R. (KBr, cm^{-1}) 3428–3224 (NH, NH_2), 1676 (CO); ^1H NMR (DMSO) δ 0.93 (t, 3H, CH_3); 1.43 (m, 2H, CH_2); 1.67 (m, 2H, CH_2); 3.94 (t, 2H, CH_2); 6.31 (s, 2H, NH_2, exchangeable); 6.89–8.18 (a set of signals, 8H, aromatic protons). 9.35 (s, 1H, NH, exchangeable). Anal. ($C_{18}H_{20}N_4O_2$) C, H, N.

*7.1.3.1.5. N-(4-Acetylphenyl)-3-amino-1H-indazole-1-carboxamide **10f***. 4-Acetylphenyl isocyanate **8f** was allowed to react with 3-aminoindazole **9** as described in Section 7.1.3.1 to give **10f**. The solid collected was crystallized from dioxane, 98% yield; mp 228–230 °C; I.R. (KBr, cm^{-1}) 3469–3185 (NH, NH_2), 1703 (CO),1660 (CO); ^1H NMR (DMSO) δ 2.55 (s, 3H, CH_3); 6.42 (s, 2H, NH_2, exchangeable); 7.28–8.22 (a set of signals, 8H, aromatic protons). 9.89 (s, 1H, NH, exchangeable) Anal. ($C_{16}H_{14}N_4O_2$) C, H, N.

*7.1.3.1.6. 3-Amino-N-(2-chloro-4-nitrophenyl)-1H-indazole-1-carboxamide **10j***. 2-Chloro-4-nitrophenyl isocyanate **8j** was allowed to react with 3-aminoindazole **9** as described in Section 7.1.3.1 to give **10j**. The solid collected was crystallized from ethanol, 22% yield; mp 191–193 °C; I.R. (KBr, cm^{-1}) 3426–3311 (NH, NH_2), 1720 (CO); ^1H NMR (DMSO) δ 6.70 (s, 2H, NH_2, exchangeable); 7.27–8.59 (a set of signals, 7H, aromatic protons). 9.70 (s, 1H, NH, exchangeable). Anal. ($C_{14}H_{10}ClN_5O_3$) C, H, N.

*7.1.3.1.7. 3-Amino-N-1-naphthyl-1H-indazole-1-carboxamide **10k***. 1-Naphthyl isocyanate **8k** was allowed to react with 3-aminoindazole **9** as described in Section 7.1.3.1 to give **10k**. The solid collected was crystallized from ethanol, yield 60%; mp 191–193 °C; I.R. (KBr, cm^{-1}) 3405–3325 (NH, NH_2), 1678 (CO); ^1H NMR (DMSO) δ 6.51 (s, 2H, NH_2, exchangeable); 7.27–8.19 (a set of signals, 11H, aromatic protons). 9.70 (s, 1H, NH, exchangeable). Anal. ($C_{14}H_{10}ClN_5O_3$) C, H, N.

*7.1.3.1.8. 3-Amino-N-(2-methyl-5-nitrophenyl)-1H-indazole-1-carboxamide **10m***. 2-Methyl-5-nitrophenyl isocyanate **8m** was allowed to react with 3-aminoindazole **9** as described in Section 7.1.3.1 to give **10m**. The solid collected was crystallized from dioxane, 74% yield; mp 250–253 °C; I.R. (KBr, cm^{-1}) 3466–3371 (NH, NH_2), 1703 (CO); ^1H NMR (DMSO) δ 2.44 (s, 3H, CH_3); 6.56 (s, 2H, NH_2, exchangeable); 7.26–8.84 (a set of signals, 7H, aromatic protons). 9.26 (s, 1H, NH, exchangeable). Anal. ($C_{15}H_{13}N_5O_3$) C, H, N.

*7.1.3.1.9. 3-Amino-N-(2-ethoxyphenyl)-1H-indazole-1-carboxamide **10r***. 2-Ethoxyphenyl isocyanate **8r** was allowed to react with 3-aminoindazole **9** as described in Section 7.1.3.1 to give **10r**. The solid collected was crystallized from ethanol, 60% yield; mp 143–145 °C; I.R. (KBr, cm^{-1}) 3423, 3348 (NH, NH_2), 1702 (CO); ^1H NMR (DMSO) δ 1.46 (t, 3H, CH_3); 4.19 (q, 2H, CH_2); 6.56 (s, 2H, NH_2, exchangeable); 6.97–8.29 (a set of signals, 8H, aromatic protons). 9.37 (s, 1H, NH, exchangeable). Anal. ($C_{16}H_{16}N_4O_2$) C, H, N.

*7.1.3.1.10. 3-Amino-N-(2-benzylphenyl)-1H-indazole-1-carboxamide **10t***. 2-Benzylphenyl isocyanate **8t** was allowed to react with 3-aminoindazole **9** as described in Section 7.1.3.1 to give **10t**. The solid collected was crystallized from ethanol, 61% yield; mp 135–136 °C; I.R. (KBr, cm^{-1}) 3442, 3374, 3353 (NH, NH_2), 1703 (CO); ^1H NMR (DMSO) δ 4.04 (s, 2H, CH_2); 6.41 (s, 2H, NH_2, exchangeable); 7.08–8.15 (a set of signals, 13H, aromatic protons). 9.06 (s, 1H, NH, exchangeable). Anal. ($C_{21}H_{18}N_4O$) C, H, N.

*7.1.3.1.11. 3-Amino-N-(2-methoxy-5-nitrophenyl)-1H-indazole-1-carboxamide **10u***. 2-Methoxy-5-nitrophenyl isocyanate **8u** was allowed to react with 3-aminoindazole **9** as described in Section 7.1.3.1 to give **10u**. The solid collected was crystallized from dioxane, 76% yield; mp 245–249 °C; I.R. (KBr, cm^{-1}) 3463–3336 (NH, NH_2), 1704 (CO); ^1H NMR (DMSO) δ 4.08 (s, 3H, OCH_3); 6.66 (s, 2H, NH_2, exchangeable); 7.28–9.15 (a set of signals, 7H, aromatic protons). 9.34 (s, 1H, NH, exchangeable). Anal. ($C_{15}H_{13}N_5O_4$) C, H, N.

*7.1.3.1.12. 3-Amino-N-(3,4-dimethoxyphenyl)-1H-indazole-1-carboxamide **10v***. 3,4-Dimethoxyphenyl isocyanate **8v** was allowed to react with 3-aminoindazole **9** as described in Section 7.1.3.1 to give **10v**. Purified by flash chromatography on silica gel [25] with chloroform as eluant, and crystallized from ethanol, 45% yield; mp 158–159 °C; I.R. (KBr, cm^{-1}) 3445–3249 (NH, NH_2), 1680 (CO); ^1H NMR (DMSO) δ 3.74 (s, 3H, OCH_3); 3.78 (s, 3H, OCH_3); 6.32 (s, 2H, NH_2, exchangeable); 6.91–8.20 (a set of signals, 7H, aromatic protons). 9.33 (s, 1H, NH, exchangeable). Anal. ($C_{16}H_{16}N_4O_3$) C, H, N.

*7.1.3.1.13. 3-Amino-N-[4-(benzyloxy)phenyl]-1H-indazole-1-carboxamide **10w***. 4-(Benzyloxy)phenyl isocyanate **8w** was allowed to react with 3-aminoindazole **9** as described in Section 7.1.3.1 to give **10w**. The solid collected was crystallized from ethanol, 95% yield; mp 127–128 °C; I.R. (KBr, cm^{-1}) 3458, 3368 (NH, NH_2), 1706 (CO); ^1H NMR (DMSO) δ 5.09 (s, 2H, OCH_2); 6.32 (s, 2H, NH_2, exchangeable); 6.99–8.19 (a set of signals, 13H, aromatic protons). 9.39 (s, 1H, NH, exchangeable). Anal. ($C_{21}H_{18}N_4O_2$) C, H, N.

*7.1.3.1.14. 3-Amino-N-(2,4-dimethoxyphenyl)-1H-indazole-1-carboxamide **10x***. 2,4-Dimethoxyphenyl isocyanate **8x** was allowed to react with 3-aminoindazole **9** as described in Section 7.1.3.1 to give **10x**. The solid collected was crystallized from ethanol, 57% yield; mp 140–142 °C; I.R. (KBr, cm^{-1}) 3412–3234 (NH, NH_2), 1686 (CO); ^1H NMR (DMSO) δ 3.78 (s, 3H, OCH_3); 3.91 (s, 3H, OCH_3); 6.52 (s, 2H, NH_2, exchangeable); 6.55–8.18 (a set of signals, 7H, aromatic protons). 8.99 (s, 1H, NH, exchangeable). Anal. ($C_{16}H_{16}N_4O_3$) C, H, N.

*7.1.3.1.15. 3-Amino-N-(2-methoxyphenyl)-1H-indazole-1-carboxamide **10y***. 2-Methoxyphenyl isocyanate **8y** was allowed to react with 3-aminoindazole **9** as described in Section 7.1.3.1 to give **10y**. Purified by flash chromatography on silica gel [25] with chloroform as eluant, and crystallized from dioxane, 89% yield; mp 163–165 °C; I.R. (KBr, cm^{-1}) 3431–3342 (NH, NH_2), 1708, 1691 (CO); ^1H NMR (DMSO) δ 3.94 (s, 3H, OCH_3); 6.59 (s, 2H, NH_2, exchangeable); 6.97–8.29 (a set of signals, 8H, aromatic protons). 9.26 (s, 1H, NH, exchangeable). Anal. ($C_{15}H_{14}N_4O_2$) C, H, N.

*7.1.3.1.16. 3-Amino-N-(2,5-dimethoxyphenyl)-1H-indazole-1-carboxamide **10z***. 2,5-Dimethoxyphenyl isocyanate **8z** was allowed to react with 3-aminoindazole **9** as described in Section 7.1.3.1 to give **10z**. The solid collected was crystallized

from dioxane, 98% yield; mp 172–176 °C; I.R. (KBr, cm^{-1}) 3450, 3352 (NH, NH_2), 1691 (CO); ^1H NMR (DMSO) δ 3.74 (s, 3H, OCH_3); 3.87 (s, 3H, OCH_3); 6.56 (s, 2H, NH_2, exchangeable); 6.59–8.20 (a set of signals, 7H, aromatic protons). 9.25 (s, 1H, NH, exchangeable). Anal. ($C_{16}H_{16}N_4O_3 \cdot 1/2H_2O$) C, H, N.

7.1.4. Synthesis of N-phenyl-3-(phenylureido)-1H-indazole-1-carboxamides **11**

7.1.4.1. General method. Substituted phenyl isocyanate **8** (14 mmol) was added drop wise to a solution of 3-aminoindazole **9** (7 mmol) in 10 ml of THF then the mixture was heated to reflux for a suitable time. After this time, the solution was concentrated under reduced pressure, the residue washed with ethanol and then crystallized from a suitable solvent.

7.1.4.1.1. N-(2,6-Difluorophenyl)-3-({[(2,6-difluorophenyl)amino]carbonyl}amino)-1H-indazole-1-carboxamide ***11a***. 2,6-Difluorophenyl isocyanate **8a** was heated to reflux with 3-aminoindazole **9** for 1 h as described in Section 7.1.4.1 to give **11a**. The solid collected was crystallized from dioxane, 30% yield; mp 201–202 °C; I.R. (KBr, cm^{-1}) 3384–3127 (NH), 1714 (CO), 1690 (CO); ^1H NMR (DMSO) δ 7.20–8.34 (a set of signals, 10H, aromatic protons); 9.42 (s, 1H, NH, exchangeable); 10.02 (s, 1H, NH, exchangeable); 10.70 (s, 1H, NH, exchangeable). Anal. ($C_{21}H_{13}F_4N_5O_2$) C, H, N.

7.1.4.1.2. N-(4-Benzylphenyl)-3-({[(4-benzylphenyl)amino]carbonyl}amino)-1H-indazole-1-carboxamide ***11d***. 4-Benzylphenyl isocyanate **8d** was heated to reflux with 3-aminoindazole **9** for 1 h as described in Section 7.1.4.1 to give **11d**. The solid collected was crystallized from ethanol, 38% yield; mp 160–163 °C; I.R. (KBr, cm^{-1}) 3410–3129 (NH), 1716 (CO), 1691 (CO); ^1H NMR (DMSO) δ 3.91 (s, 2H, CH_2); 3.93 (s, 2H, CH_2); 7.20–8.30 (a set of signals, 22H, aromatic protons); 9.76 (s, 1H, NH, exchangeable); 10.10 (s, 2H, 2 × NH, exchangeable). Anal. ($C_{35}H_{29}N_5O_2 \cdot 1/2H_2O$) C, H, N.

7.1.4.1.3. N-(4-Butoxyphenyl)-3-({[(4-butoxyphenyl)amino]carbonyl}amino)-1H-indazole-1-carboxamide ***11e***. 4-Butoxyphenyl isocyanate **8e** was heated to reflux with 3-aminoindazole **9** for 1 h as described in Section 7.1.4.1 to give **11e**. The solid collected was crystallized from dioxane, 23% yield; mp 225–229 °C; I.R. (KBr, cm^{-1}) 3311–3130 (NH), 1687 (br, CO); ^1H NMR (DMSO) δ 0.93 (t, 6H, 2 × CH_3); 1.44 (q, 4H, 2 × CH_2); 1.63–1.73 (m, 4H, 2 × CH_2); 3.95 (q, 4H, 2 × CH_2); 6.91–8.30 (a set of signals, 12H, aromatic protons). 9.70 (s, 1H, NH, exchangeable); 10.08 (s, 1H, NH, exchangeable); 10.11 (s, 1H, NH, exchangeable). Anal. ($C_{29}H_{33}N_5O_4$) C, H, N.

7.1.4.1.4. N-(4-Acetylphenyl)-3-({[(4-acetylphenyl)amino]carbonyl}amino)-1H-indazole-1-carboxamide ***11f***. 4-Acetylphenyl isocyanate **8f** was heated to reflux with 3-aminoindazole **9** for 1 h as described in Section 7.1.4.1 to give **11f**. The solid collected was crystallized from dioxane, 23% yield; mp 250–253 °C; I.R. (KBr, cm^{-1}) 3270–3116 (NH), 1715 (CO), 1672 (CO); ^1H NMR (DMSO) δ 2.54 (s, 6H, 2 × CH_3); 7.38–8.31 (a set of signals, 12H, aromatic protons); 10.11 (s, 1H, NH, exchangeable); 10.26 (s, 1H, NH, exchangeable); 10.47 (s, 1H, NH, exchangeable). Anal. ($C_{25}H_{21}N_5O_4$) C, H, N.

7.1.4.1.5. N-(4-Methoxyphenyl)-3-({[(4-methoxyphenyl)amino]carbonyl}amino)-1H-indazole-1-carboxamide ***11g***. 4-Methoxyphenyl isocyanate **8g** was heated to reflux with 3-aminoindazole **9** for 1 h as described in Section 7.1.4.1 to give **11g**. The solid collected was crystallized from dioxane, 27% yield; mp 240–242 °C; I.R. (KBr, cm^{-1}) 3412–3127 (NH), 1687 (br, CO); ^1H NMR (DMSO) δ 3.75 (s, 3H, OCH_3); 3.77 (s, 3H, CH_3); 6.93–8.31 (a set of signals, 12H, aromatic protons); 9.72 (s, 1H, NH, exchangeable); 10.10 (s, 2H, 2 × NH, exchangeable). Anal. ($C_{23}H_{21}N_5O_4$) C, H, N.

7.1.4.1.6. N-(4-Trifluoromethoxyphenyl)-3-({[(4-(trifluoromethoxy)phenyl)amino]carbonyl}amino)-1H-indazole-1-carboxamide ***11h***. 4-(Trifluoromethoxy)phenyl isocyanate **8h** was heated to reflux with 3-aminoindazole **9** for 1 h and 30 min as described in Section 7.1.4.1 to give **11h**. The solid collected was crystallized from dioxane, 36% yield; mp 257–261 °C; I.R. (KBr, cm^{-1}) 3417–3135 (NH), 1718 (CO), 1690 (CO); ^1H NMR (DMSO) δ 7.36–8.33 (a set of signals, 12H, aromatic protons); 9.96 (s, 1H, NH, exchangeable); 10.25 (s, 1H, NH, exchangeable); 10.38 (s, 1H, NH, exchangeable).Anal. ($C_{23}H_{15}F_6N_5O_4$) C, H, N.

7.1.4.1.7. N-(2-Fluoro-5-trifluoromethylphenyl)-3-({[(2-fluoro-5-(trifluoromethyl)phenyl)amino]carbonyl}amino)-1H-indazole-1-carboxamide ***11i***. 2-Fluoro-5-(trifluoromethyl) phenyl isocyanate **8i** was heated to reflux with 3-aminoindazole **9** for 1 h as described in Section 7.1.4.1 to give **11i**. The solid collected was crystallized from ethanol, 15% yield; mp 250–252 °C; I.R. (KBr, cm^{-1}) 3408–3146 (NH), 1701 (br, CO); ^1H NMR (DMSO) δ 7.38–8.53 (a set of signals, 10H, aromatic protons); 9.79 (br s, 1H, NH, exchangeable); 9.88 (br s, 1H, NH, exchangeable); 10.52 (br s, 1H, NH, exchangeable).Anal. ($C_{23}H_{13}F_8N_5O_2$) C, H, N.

7.1.4.1.8. N-(2-Trifluoromethoxyphenyl)-3-({[(2-trifluoromethoxyphenyl)amino]carbonyl}amino)-1H-indazole-1-carboxamide ***11l***. 2-(Trifluoromethoxy)phenyl isocyanate **8l** was heated to reflux with 3-aminoindazole **9** for 3 h as described in Section 7.1.4.1 to give **11l**. The solid collected was crystallized from ethanol, 35% yield; mp 195–200 °C; I.R.(KBr, cm^{-1}) 3418–3141 (NH), 1722 (CO), 1689 (CO); ^1H NMR (DMSO) δ 7.25–8.31 (a set of signals, 12H, aromatic protons); 9.64 (s, 1H, NH, exchangeable); 9.72 (s, 1H, NH, exchangeable); 10.50 (s, 1H, NH, exchangeable).Anal. ($C_{23}H_{15}F_6N_5O_4$) C, H, N.

7.1.4.1.9. N-(3,4-Dichlorophenyl)-3-({[(3,4-dichlorophenyl)amino]carbonyl}amino)-1H-indazole-1-carboxamide ***11n***. 3,4-Dichlorophenyl isocyanate **8n** was heated to reflux for 10 min with 3-aminoindazole **9** then stirred at room temperature for 24 h as described in Section 7.1.4.1 to give **11n**. The solid collected was washed with ethanol and crystallized from dioxane, 98% yield; mp 268–270 °C; I.R. (KBr, cm^{-1}) 3419–3122 (NH), 1727 (CO), 1696 (CO); ^1H NMR (DMSO) δ 7.36–8.30 (a set of signals, 10H, aromatic protons); 10.01 (br s, 1H, NH, exchangeable); 10.32 (br s, 1H,

NH, exchangeable); 10.44 (br s, 1H, NH, exchangeable). Anal. ($C_{21}H_{13}Cl_4N_5O_2$) C, H, N.

7.1.4.1.10. N-(4-Bromophenyl)-3-({[(4-bromophenyl)amino]carbonyl}amino)-1H-indazole-1-carboxamide ***11q***. 4-Bromophenyl isocyanate **8q** was heated to reflux with 3-aminoindazole **9** for 1 h as described in Section 7.1.4.1 to give **11q**. The solid collected was crystallized from *N*,*N*,-dimethylformamide, 60% yield; mp 278–280 °C; I.R. (KBr, cm^{-1}) 3415–3120 (NH), 1692 (CO), 1681 (CO); ^{1}H NMR (DMSO) δ 7.36–8.32 (a set of signals, 12H, aromatic protons); 9.88 (s, 1H, NH, exchangeable); 10.17 (s, 1H, NH, exchangeable); 10.27 (s, 1H, NH, exchangeable). Anal. ($C_{21}H_{15}Br_2N_5O_2$) C, H, N.

7.1.4.1.11. N-(2-Ethoxyphenyl)-3-({[(2-ethoxyphenyl)amino]carbonyl}amino)-1H-indazole-1-carboxamide ***11r***. 2-Ethoxyphenyl isocyanate **8r** was heated to reflux with 3-aminoindazole **9** for 3 h as described in Section 7.1.4.1 to give **11r**. The solid collected was crystallized from dioxane, 30% yield; mp 241–243 °C; I.R. (KBr, cm^{-1}) 3394–3111 (NH), 1716 (CO), 1683 (CO); ^{1}H NMR (DMSO) δ 1.04 (t, 3H, CH_3);1.21 (t, 3H, CH_3); 3.97–4.07 (m, 4H, $2 \times CH_2$); 6.97–8.34 (a set of signals, 12H, aromatic protons); 9.38 (s, 1H, NH, exchangeable); 9.67 (s, 1H, NH, exchangeable); 10.51 (s, 1H, NH, exchangeable). Anal. ($C_{25}H_{25}N_5O_4$) C, H, N.

7.1.4.1.12. N-(4-Butylphenyl)-3-({[(4-butylphenyl)amino]carbonyl}amino)-1H-indazole-1-carboxamide ***11s***. 4-Butylphenyl isocyanate **8s** was heated to reflux with 3-aminoindazole **9** for 3 h as described in Section 7.1.4.1 to give **11s**. The solid collected was crystallized from dioxane, 32% yield; mp 238–241 °C; I.R. (KBr, cm^{-1}) 3417–3126 (NH), 1723 (CO), 1690 (CO); ^{1}H NMR (DMSO) δ 0.89 (t, 6H, $2 \times CH_3$); 1.27–1.35 (m, 4H, $2 \times CH_2$); 1.52–1.62 (m, 4H, $2 \times CH_2$); 2.52–2.59 (m, 4H, $2 \times CH_2$); 7.15–8.32 (a set of signals, 12H, aromatic protons); 9.78 (s, 1H, NH, exchangeable); 10.09 (s, 1H, NH, exchangeable); 10.12 (s, 1H, NH, exchangeable). Anal. ($C_{29}H_{33}N_5O_2$) C, H, N.

7.1.5. Synthesis of 1-(1H-indazol-3-yl)-3-phenylureidic derivatives ***12***

7.1.5.1. General methods. Method A. Substituted *N*-Phenyl-3-(phenylureido)-1*H*-indazole-1-carboxamide **11** (1.16 mmol) was dissolved in 50 ml of ethanol and heated to reflux for 10 min. After this time 50 ml of 2 N NaOH was added and the reflux resumed for 15 min. At the completion of the reaction the ethanol was removed under reduced pressure, the mixture cooled at room temperature in ice bath and the pH adjusted to 4.0 with aqueous concentrated HCl. The solid was filtered, washed first with water then with ethanol before being recrystallized from a suitable solvent.

Method B. A mixture of 14 mmol of substituted phenyl isocyanates **8** and 14 mmol of 3-aminoindazole **9** in 10 ml of THF was heated to reflux for 3 h. At the completion of the reaction the solvent was removed under reduced pressure, washed with hot ethanol and recrystallized from a suitable solvent.

7.1.5.1.1. N-(2,6-Difluorophenyl)-N′-(1H-indazol-3-yl)urea ***12a***. *N*-(2,6-Difluorophenyl)-3-({[(2,6-difluorophenyl)amino]carbonyl}amino)-1*H*-indazole-1-carboxamide **11a** was hydrolyzed as described in Section 7.1.5.1 (*Method A*) to give **12a**. The solid collected was crystallized from dioxane, 52% yield; mp 216–218 °C; I.R. (KBr, cm^{-1}) 3278 (br, NH), 1651 (CO); ^{1}H NMR (DMSO) δ 7.07–7.99 (a set of signals, 7H, aromatic protons); 9.38 (s, 1H, NH, exchangeable); 9.88 (s, 1H, NH, exchangeable); 12.54 (s, 1H, NH, exchangeable). Anal. ($C_{14}H_{10}F_2N_4O$) C, H, N.

7.1.5.1.2. N-(2,5-Dichlorophenyl)-N′-(1H-indazol-3-yl)urea ***12b***. 2,5-Dichlorophenyl isocyanate **8b** was allowed to react with 3-aminoindazole **9** as described in Section 7.1.5.1 (*Method B*) to give **12b**. Purified by flash chromatography on silica gel [25] with chloroform as eluant, and crystallized from ethanol, 96% yield; mp 188–189 °C; I.R. (KBr, cm^{-1}) 3406–3225 (br, NH), 1694 (CO); ^{1}H NMR (DMSO) δ 7.07–8.51 (a set of signals, 7H, aromatic protons); 10.30 (s, 1H, NH, exchangeable); 10.70 (s, 1H, NH, exchangeable); 12.68 (s, 1H, NH, exchangeable). Anal. ($C_{14}H_{10}Cl_2N_4O$) C, H, N.

7.1.5.1.3. N-(4-Phenoxyphenyl)-N′-(1H-indazol-3-yl)urea ***12c***. 4-Phenoxyphenyl isocyanate **8c** was allowed to react with 3-aminoindazole **9** as described in Section 7.1.5.1 (*Method B*) to give **12c**. The solid collected was crystallized from dioxane, 21% yield; mp 212–214 °C; I.R. (KBr, cm^{-1}) 3369–3092 (NH), 1692 (CO); ^{1}H NMR (DMSO) δ 6.98–8.03 (a set of signals, 13H, aromatic protons); 9.61 (s, 1H, NH, exchangeable); 9.94 (s, 1H, NH, exchangeable); 12.53 (s, 1H, NH, exchangeable). Anal. ($C_{20}H_{16}N_4O_2$) C, H, N.

7.1.5.1.4. N-(4-Benzylphenyl)-N′-(1H-indazol-3-yl)urea ***12d***. *N*-(4-Benzylphenyl)-3-({[(4-benzylphenyl)amino]carbonyl}amino)-1*H*-indazole-1-carboxamide **11d** was hydrolyzed as described in Section 7.1.5.1 (*Method A*) to give **12d**. The solid residue collected was crystallized from dioxane, 98% yield; mp 236–238 °C; I.R. (KBr, cm^{-1}) 3291–3140 (NH), 1686 (br CO); ^{1}H NMR (DMSO) δ 3.90 (s, 2H, CH_2); 7.06–8.03 (a set of signals, 13H, aromatic protons); 9.57 (s, 1H, NH, exchangeable); 9.88 (s, 1H, NH, exchangeable); 12.51 (s, 1H, NH, exchangeable). Anal. ($C_{21}H_{18}N_4O$) C, H, N.

7.1.5.1.5. N-(4-Butoxyphenyl)-N′-(1H-indazol-3-yl)urea ***12e***. *N*-(4-Butoxyphenyl)-3-({[(4-butoxyphenyl)amino]carbonyl}amino)-1*H*-indazole-1-carboxamide **11e** was hydrolyzed as described in Section 7.1.5.1 (*Method A*) to give **12e**. The solid collected was crystallized from ethanol, 98% yield; mp 216–217 °C; I.R. (KBr, cm^{-1}) 3349–3145 (NH), 1676 (CO); ^{1}H NMR (DMSO) δ 0.93 (t, 3H, CH_3); 1.38–1.48 (m, 2H, CH_2); 1.65–1.71 (m, 2H, CH_2); 3.92 (t, 2H, CH_2); 6.88–8.06 (a set of signals, 8H, aromatic protons); 9.59 (s, 1H, NH, exchangeable); 9.85 (s, 1H, NH, exchangeable); 12.50 (s, 1H, NH, exchangeable). Anal. ($C_{18}H_{20}N_4O_2$) C, H, N.

7.1.5.1.6. N-(4-Acetylphenyl)-N′-(1H-indazol-3-yl)urea ***12f***. *N*-(4-Acetylphenyl)-3-({[(4-acetylphenyl)amino]carbonyl}-amino)-1*H*-indazole-1-carboxamide **11f** was hydrolyzed as described in Section 7.1.5.1 (*Method A*) to give **12f**. The solid collected was crystallized from dioxane, 95% yield; mp 252–254 °C; I.R. (KBr, cm^{-1}) 3305–3101 (NH), 1671 (CO), 1700 (CO); ^{1}H NMR (DMSO) δ 2.53 (s, 3H, CH_3); 7.05–8.02 (a set of signals, 8H, aromatic protons); 9.68 (s, 1H, NH, exchangeable); 10.14 (s, 1H, NH, exchangeable);

12.60 (s, 1H, NH, exchangeable). Anal. ($C_{16}H_{14}N_4O_2$) C, H, N.

7.1.5.1.7. N-(4-Methoxyphenyl)-N′-(1H-indazol-3-yl)urea ***12g***. *N*-(4-Methoxyphenyl)-3-({[(4-methoxyphenyl)amino] carbonyl}amino)-1*H*-indazole-1-carboxamide **11g** was hydrolyzed as described in Section 7.1.5.1 (*Method A*) to give **12g**. The solid collected was crystallized from ethanol, 88% yield; mp 228–230 °C; I.R. (KBr, cm^{-1}) 3325–3089 (NH), 1671 (CO); ^1H NMR (DMSO) δ 3.73 (s, 3H, OCH_3); 6.89–8.05 (a set of signals, 8H, aromatic protons); 9.52 (s, 1H, NH, exchangeable); 9.79 (s, 1H, NH, exchangeable); 12.47 (s, 1H, NH, exchangeable). Anal. ($C_{15}H_{14}N_4O_2$) C, H, N.

7.1.5.1.8. N-[4-(Trifluoromethoxy)phenyl]-N′-(1H-indazol-3-yl)urea ***12h***. *N*-(4-(Trifluoromethoxy)phenyl)-3-({[(4-(trifluoromethoxy)phenyl)amino]carbonyl}amino)-1*H*-indazole-1-carboxamide **11h** was hydrolyzed as described in Section 7.1.5.1 (*Method A*) to give **12h**. The solid collected was crystallized from ethanol, 98% yield; mp 241–245 °C; I.R. (KBr, cm^{-1}) 3448–3127 (NH), 1692 (CO); ^1H NMR (DMSO) δ 7.31–7.67 (a set of signals, 8H, aromatic protons); 9.64 (s, 1H, NH, exchangeable); 10.00 (s, 1H, NH, exchangeable); 12.57 (s, 1H, NH, exchangeable). Anal. ($C_{15}H_{11}F_3N_4O_2$) C, H, N.

7.1.5.1.9. N-[2-Fluoro-5-(trifluoromethyl)phenyl]-N′-(1H-indazol-3-yl)urea ***12i***. *N*-(4-(Trifluoromethoxy)phenyl)-3-({[(4-(trifluoromethoxy)phenyl)amino]carbonyl}amino)-1*H*-indazole-1-carboxamide **11i** was hydrolyzed as described in Section 7.1.5.1 (*Method A*) to give **12i**. The solid collected was crystallized from dioxane, 98% yield; mp 220–222 °C; I.R. (KBr, cm^{-1}) 3402–3140 (NH), 1674 (CO); ^1H NMR (DMSO) δ 7.07–8.75 (a set of signals, 7H, aromatic protons); 10.12 (s, 1H, NH, exchangeable); 10.54 (br s, 1H, NH, exchangeable); 12.69 (s, 1H, NH, exchangeable). Anal. ($C_{15}H_{10}F_4N_4O$) C, H, N.

7.1.5.1.10. N-[2-(Trifluoromethoxy)phenyl]-N′-(1H-indazol-3-yl)urea ***12l***. *N*-(2-(Trifluoromethoxy)phenyl)-3-({[(2-(trifluoromethoxy)phenyl)phenylamino]carbonyl}amino)-1*H*-indazole-1-carboxamide **11l** was hydrolyzed as described in Section 7.1.5.1 (*Method A*) to give **12l**. The solid collected was crystallized from ethanol, 98% yield; mp 192 °C; I.R. (KBr, cm^{-1}) 3300 (br, NH), 1665 (CO); ^1H NMR (DMSO) δ 7.06–8.45 (a set of signals, 8H, aromatic protons); 10.18 (br s, 1H, NH, exchangeable); 10.72 (br s, 1H, NH, exchangeable); 12.58 (br s, 1H, NH, exchangeable). Anal. ($C_{15}H_{11}F_3N_4O_2$) C, H, N.

7.1.5.1.11. N-(3,4-Dichlorophenyl)-N′-(1H-indazol-3-yl)urea ***12n***. *N*-(3,4-Dichlorophenyl)-3-({[(3,4-dichlorophenyl)amino]carbonyl}amino)-1*H*-indazole-1-carboxamide **11n** was hydrolyzed as described in Section 7.1.5.1 (*Method A*) to give **12n**. The solid collected was crystallized from ethanol, 98% yield; mp 244–250 °C; I.R. (KBr, cm^{-1}) 3439–3122 (NH), 1693 (CO); ^1H NMR (DMSO) δ 7.08–7.98 (a set of signals, 7H, aromatic protons); 9.67 (s, 1H, NH, exchangeable); 9.99 (s, 1H, NH, exchangeable); 12.58 (s, 1H, NH, exchangeable). Anal. ($C_{14}H_{10}Cl_2N_4O$) C, H, N.

7.1.5.1.12. N-(4-Nitrophenyl)-N′-(1H-indazol-3-yl)urea ***12o***. 4-Nitrophenyl isocyanate **8o** was allowed to react with 3-aminoindazole **9** as described in Section 7.1.5.1 (*Method B*) to give **12o**. The solid collected was crystallized from DMF/H_2O, 40% yield; mp 288–290 °C; I.R. (KBr, cm^{-1}) 3397–3086 (NH), 1698 (CO); ^1H NMR (DMSO) δ 7.08–8.26 (a set of signals, 8H, aromatic protons); 9.75 (s, 1H, NH, exchangeable); 10.31 (s, 1H, NH, exchangeable); 12.67 (s, 1H, NH, exchangeable). Anal. ($C_{14}H_{11}N_5O_3$) C, H, N.

7.1.5.1.13. N-(2-Methyl-4-nitrophenyl)-N′-(1H-indazol-3-yl)urea ***12p***. 2-Methyl-4-nitrophenyl isocyanate **8p** was allowed to react with 3-aminoindazole **9** as described in Section 7.1.5.1 (*Method B*) to give **12p**. The solid collected was crystallized from DMF, 75% yield; mp 264–265 °C; I.R. (KBr, cm^{-1}) 3479–3334 (NH), 1704 (CO); ^1H NMR (DMSO) δ 2.48 (s, 3H, CH_3); 7.06–8.55 (a set of signals, 7H, aromatic protons); 10.27 (s, 1H, NH, exchangeable); 10.50 (br s, 1H, NH, exchangeable); 12.69 (s, 1H, NH, exchangeable). Anal. ($C_{15}H_{13}N_5O_3$) C, H, N.

7.1.5.1.14. N-(4-Bromophenyl)-N′-(1H-indazol-3-yl)urea ***12q***. *N* -(4-Bromophenyl)-3-({[(4-bromophenyl)amino]carbonyl}amino)-1*H*-indazole-1-carboxamide **11q** was hydrolyzed as described in Section 7.1.5.1 (*Method A*) to give **12q**. The solid collected was crystallized from ethanol, 90% yield; mp 235–237 °C; I.R. (KBr, cm^{-1}) 3429–3115 (NH), 1689 (CO); ^1H NMR (DMSO) δ 7.05–8.03 (a set of signals, 8H, aromatic protons); 9.64 (s, 1H, NH, exchangeable); 9.97 (s, 1H, NH, exchangeable); 12.56 (s, 1H, NH, exchangeable). Anal. ($C_{14}H_{11}BrN_4O$) C, H, N.

7.1.5.1.15. N-(2-Ethoxyphenyl)-N′-(1H-indazol-3-yl)urea ***12r***. *N* -(2-Ethoxyphenyl)-3-({[(2-ethoxyphenyl)amino]carbonyl}amino)-1*H*-indazole-1-carboxamide **11r** was hydrolyzed as described in Section 7.1.5.1 (*Method A*) to give **12r**. The solid collected was crystallized from ethanol, 93% yield; mp 182–183 °C; I.R. (KBr, cm^{-1}) 3333–3131 (NH), 1678 (CO); ^1H NMR (DMSO) δ 1.50 (t, 3H, CH_3); 4.12 (q, 2H, CH_2); 6.63–8.31 (a set of signals, 8H, aromatic protons); 10.00 (s, 1H, NH, exchangeable); 10.61 (br s, 1H, NH, exchangeable); 12.48 (s, 1H, NH, exchangeable). Anal. ($C_{16}H_{16}N_4O_2$) C, H, N.

7.2. X-ray structure determination

Crystals of **10w** were obtained from an ethanol solution at room temperature as yellow prisms. The intensity data were collected on Enraf Nonius CAD-4 diffractometer with Mo Kα radiation ($\lambda = 0.71073$(Å)) at room temperature. The lattice parameters were determined by least-squares refinements of 25 high angle reflections. Crystal system: monoclinic (*I*2/*c*), cell dimensions (Å) $a = 23.227(4)$, $b = 5.801(1)$, $c = 27.825(5)$, $\beta = 111.76(2)^\circ$, Final R indices $[I > 2\sigma(I)]$ $R_1 = 0.088$, $wR_2 = 0.178$ for 3205 independent reflections. The structure was solved by direct methods and the refinement was carried out with SHELX-97 [26]. All non-H-atoms were refined anisotropically. The H-atoms positions were detected in a difference Fourier synthesis and refined with isotropic thermal factors.

CCDC-644638 contains the supplementary crystallographic data for this paper. These data can be obtained free of charge via www.ccdc.cam.ac.uk/conts/retrieving.html (or from the

Cambridge Crystallographic Data Centre, 12, Union Road, Cambridge CB21EZ, UK; fax: +44 1223 336 033; or deposit@ccdc.cam.ac.uk).

7.3. Biology

7.3.1. Methodology of the in vitro cancer screen

The human tumor cell lines of the cancer screening panel are grown in RPMI 1640 medium containing 5% foetal bovine serum and 2 mM L-glutamine. For a typical screening experiment, cells are inoculated into 96 well microtiter plates in 100 μl at plating densities ranging from 5,000 to 40,000 cells/well depending on the doubling time of individual cell lines. After cell inoculation, the microtiter plates are incubated at 37 °C, 5% CO_2, 95% air and 100% relative humidity for 24 h prior to addition of experimental drugs. After 24 h, two plates of each cell line are fixed *in situ* with TCA, to represent a measurement of the cell population for each cell line at the time of drug additions (T_z). Experimental drugs are solubilized in dimethyl sulfoxide at 400-fold the desired final maximum test concentration and stored frozen prior to use. At the time of drug addition, an aliquot of frozen concentrate is thawed and diluted to twice the desired final maximum test concentration with complete medium containing 50 μg/ml gentamicin. Additional four, 10-fold or 1/2 log serial dilutions are made to provide a total of five drug concentrations plus control. Aliquots of 100 μl of these different drug dilutions are added to the appropriate microtiter wells already containing 100 μl of medium, resulting in the required final drug concentrations. Following drug addition, the plates are incubated for an additional 48 h at 37 °C, 5% CO2, 95% air, and 100% relative humidity. For adherent cells, the assay is terminated by the addition of cold TCA. Cells are fixed *in situ* by the gentle addition of 50 μl of cold 50% (w/v) TCA (final concentration, 10% TCA) and incubated for 60 min at 4 °C. The supernatant is discarded, and the plates are washed five times with tap water and air dried. Sulforhodamine B (SRB) solution (100 μl) at 0.4% (w/v) in 1% acetic acid is added to each well, and plates are incubated for 10 min at room temperature. After staining, unbound dye is removed by washing five times with 1% acetic acid and the plates are air dried. Bound stain is subsequently solubilized with 10 mM trizma base, and the absorbance is read on an automated plate reader at a wavelength of 515 nm. For suspension cells, the methodology is the same except that the assay is terminated by fixing settled cells at the bottom of the wells by gently adding 50 μl of 80% TCA (final concentration, 16% TCA). Using the seven absorbance measurements [time zero, (T_z), control growth, C, and test growth in the presence of drug at the five concentration levels (T_i)], the percentage growth is calculated at each of the drug concentrations levels. Percentage growth inhibition is calculated as:

$[(T_i - T_z)/(C - T_z)] \times 100$ for concentrations for which $T_i \geq T_z$

$[(T_i - T_z)/T_z] \times 100$ for concentrations for which $T_i < T_z$.

Three dose response parameters are calculated for each experimental agent. Growth inhibition of 50% (GI_{50}) is calculated from $[(T_i - T_z)/(C - T_z)] \times 100 = 50$, which is the drug concentration resulting in a 50% reduction in the net protein increase (as measured by SRB staining) in control cells during the drug incubation. The drug concentration resulting in total growth inhibition (TGI) is calculated from $T_i = T_z$. The LC_{50} (concentration of drug resulting in a 50% reduction in the measured protein at the end of the drug treatment as compared to that at the beginning) indicating a net loss of cells following treatment is calculated from $[(T_i - T_z)/T_z] \times 100 = -50$. Values are calculated for each of these three parameters if the level of activity is reached; however, if the effect is not reached or is exceeded, the value for that parameter is expressed as greater or less than the maximum or minimum concentration tested.

7.3.2. Flow cytometric analysis of cell cycle distribution

The effects of the most active compounds of the series on cell cycle distribution were studied on K562 cells (myeloblastic leukemia) by flow cytometric analysis after staining with propidium iodide. Cells were exposed for 24 h to each compound. After treatment cells were washed once in ice-cold phosphate buffered saline medium (PBS − Sigma) and resuspended at 1×10^6 ml in a hypotonic fluorochrome solution containing propidium iodide (Sigma, St. Louis, Mo) 50 μg/ml in 0.1% sodium citrate plus 0.03% (v/v) nonidet P-40 (Sigma). After 30 min of incubation, the fluorescence of each sample was analyzed as single-parameter frequency histograms by using a FACScan flow cytometer (Becton Dickinson, San Jose, CA). The distribution of cells in the cell cycle was analyzed with the ModFit LT3 program (Verity Software House, Inc.).

7.3.3. Flow cytometric evaluation of pRb

Cells (1.5×10^6) were washed twice with PBS (Sigma) and resuspended in 100 μl Cytofix/Cytoperm solution (Becton Dickinson). After 20 min cells were washed twice with BD Perm/Wash ™ buffer solution (Becton Dickinson) and incubated with 20 μl FITC conjugated anti-pRb or Pe conjugated anti-underphosphorylated pRb monoclonal antibodies (Becton Dickinson) at 4 °C. After 30 min cells were washed twice and analysed by flow cytometry.

Acknowledgement

Financial support from MIUR (PRIN 2004) and MIUR (PRIN 2006) is gratefully acknowledged. The NCI Cell results were obtained through screening services provided by the Developmental Therapeutics Program of the National Cancer Institute; additional information can be found at http://dpt.nci.nih.gov/.

References

[1] Li-Jiau Huang, Mei-Ling Shih, Hua-Sin Chen, Shiow-Lin Pan, Che-Ming Teng, Lee Fang-Yu, Kuo Sheng-Chu, Bioorg. Med. Chem. 14 (2006) 528–536.
[2] L. Bouissane, S. El Kazzouli, S. Le'once, B. Pfeiffer, E.M. Rakib, M. Khouili, G. Guillaumet, Bioorg. Med. Chem. 14 (2006) 1078–1088.
[3] Y. Dai, K. Hartandi, Z. Ji, A.A. Ahmed, D.H. Albert, J.L. Bauch, J.J. Bouska, P.F. Bousquet, G.A. Cunha, K.B. Glaser, C.M. Harris, D. Hickman, J. Guo, J. Li, P.A. Marcotte, K.C. Marsh, M.D. Moskey,

R.L. Martin, A.M. Olson, D.J. Osterling, L.J. Pease, N.B. Soni, K.D. Stewart, V.S. Stoll, P. Tapang, D.R. Reuter, S.K. Davidsen, M.R. Michaelides, J. Med. Chem. 50 (2007) 1584–1597.
[4] T. Yakaiah, B.P.V. Lingaiah, B. Narsaiah, B. Shireesha, B. Ashok Kumar, S. Gururaj, T. Parthasarathy, B. Sridhar, Bioorg. Med. Chem. Lett. 17 (2007) 3445–3453.
[5] M. Fanciulli, A. Valentini, T. Bruno, G. Citro, G. Zupi, A. Floridi, Oncol. Res. 8 (1996) 111–120.
[6] G. Daidone, S. Plescia, D. Raffa, D. Schillaci, B. Maggio, F. Benetollo, G. Bombieri, Heterocycles 43 (1996) 2385–2396.
[7] D. Raffa, G. Daidone, B. Maggio, D. Schillaci, F. Plescia, Arch. Pharm. Pharm. Med. Chem. 332 (1999) 317–320.
[8] G. Daidone, D. Raffa, B. Maggio, M.V. Raimondi, F. Plescia, D. Schillaci, Eur. J. Med. Chem. 39 (2004) 219–224.
[9] V.S. Lucas, A.T. Huang, Chemotherapy of Melanoma, in: H.F. Siegel (Ed.), Development in Oncology, vol. 5, Martinus Nijhoff, The Hague, The Netherlands, 1982, p. 382.
[10] C. Chia-Hui, L. Man-Kit, S. Jen-Kuan, L. Gene-Hsiang, L. Yi-Hung, W. Yu, J. Org. Chem. 69 (2004) 1866–1871.
[11] A. Reissert, F. Graube, Berichte 42 (1909) 3710–3721.
[12] C.K. Johnson, ORTEP 11, Report ORNL-5138, Oak Ridge National Laboratory, TN, 1976.
[13] M.R. Boyd, K.D. Paull, Drug Dev. Res. 34 (1995) 91–109.
[14] R.A. Weinberg, Cell 81 (1995) 323–330.
[15] M. Korenjak, A. Brehm Curr, Opin. Genet. Dev. 15 (2005) 520–527.
[16] M. Von Willebrand, E. Zacksenhaus, E. Cheng, P. Glazer, R. Halaban, Cancer Res. 63 (2003) 1420–1429.
[17] J.R. Nevins, Hum. Mol. Genet. 10 (2001) 699–703.
[18] B. Chauffert, M.T. Dimanche-Boitrel, C. Garrido, M. Ivarsson, M. Martin, F. Martin, E. Solary, Cytotechnology 27 (1998) 225–235.
[19] F. Valeriote, L. Van Putten, Cancer Res. 3 (1975) 2619–2630.
[20] I.F. Tannock, Cancer Treat. Rep. 62 (1978) 1117–1133.
[21] P.L. Olive, R.E. Durand, Cancer Metastasis Rev. 13 (1994) 121–138.
[22] G. Toffoli, G. Corona, M. Gigante, M. Boiocchi, Eur. J. Cancer 32 (1996) 1591–1597.
[23] J. Zhou, M.A. Goldwasser, A. Li, S.E. Dahlberg, D. Neuberg, H. Wang, V. Dalton, K.D. McBride, S.E. Sallan, L.B. Silverman, J.G. Gribben, For the Dana-Farber Cancer Institute ALL Consortium DFCI ALL consortium protocol 95-01, Blood 110 (2007) 1607–1611.
[24] T. Raff, N. Gokbuget, S. Luschen, R. Reutzel, M. Ritgen, S. Irmer, S. Bottcher, H.A. Horst, M. Kneba, D. Hoelzer, M. Bruggemann, For the GMALL study group, data from the GMALL 06/99 and 07/03 trials, Blood 109 (2007) 910–915.
[25] W.C. Still, M. Kahn, A. Mitra, J. Org. Chem. 43 (1978) 2923–2925.
[26] G.M. Sheldrick, SHELX-97, University of Göttingen, Germany, 1997.